TRANSIENT MHD COUETTE FLOW OF A CASSON FLUID BETWEEN PARALLEL PLATES WITH HEAT TRANSFER

Hazem Ali Attia

Mohamed Eissa Sayed-Ahmed

Department of Engineering Mathematics and Physics
Faculty of Engineering
Fayoum University
Egypt

Abstract. The unsteady magnetohydrodynamic flow of an electrically conducting viscous incompressible non-Newtonian Casson fluid bounded by two parallel non-conducting porous plates is studied with heat transfer considering the Hall effect. An external uniform magnetic field is applied perpendicular to the plates and the fluid motion is subjected to a uniform suction and injection. The lower plate is stationary and the upper plate is suddenly set into motion and simultaneously suddenly isothermally heated to a temperature other than the lower plate temperature. Numerical solutions are obtained for the governing momentum and energy equations taking the Joule and viscous dissipations into consideration. The effect of the Hall term, the parameter describing the non-Newtonian behavior, and the velocity of suction and injection on both the velocity and temperature distributions are studied.

Keywords: MHD flow, heat transfer, non-Newtonian fluids, Hall effect, numerical solution.

1. Introduction

The study of Couette flow in a rectangular channel of an electrically conducting viscous fluid under the action of a transversely applied magnetic field has immediate applications in many devices such as magnetohydrodynamic (MHD) power generators, MHD pumps, accelerators, aerodynamics heating, electrostatic precipitation, polymer technology, petroleum industry, purification of crude oil and fluid droplets sprays. Channel flows of a Newtonian fluid with heat transfer have been studied with or without Hall currents by many authors [1]-[10]. These results are important for the design of the duct wall and the cooling arrangements. The most important non-Newtonian fluid possessing a yield value is the Casson fluid, which has significant applications in polymer processing industries and biomechanics. Casson fluid is a shear thinning liquid which has an infinite viscosity at a zero rate of shear, a yield stress below which no flow occurs and a

zero viscosity at an infinite rate of shear. Casson's constitute equation represents a nonlinear relationship between stress and rate of strain and has been found to be accurately applicable to silicon suspensions, suspensions of bentonite in water and lithographic varnishes used for printing inks [11]-[13]. Many authors [14]-[16] studied the flow or/and heat transfer of a Casson fluid in different geometries. Attia [10] has studied the influence of the Hall current on the velocity and temperature fields of an unsteady Hartmann flow of a conducting Newtonian fluid between two infinite non-conducting horizontal parallel and porous plates. The extension of such problem to the case of Couettee flow of non-Newtonian Casson fluid is done in the present study. The upper plate is moving with a uniform velocity while the lower plate is stationary. The fluid is acted upon by a constant pressure gradient, a uniform suction from above, and a uniform injection from below and is subjected to a uniform magnetic field perpendicular to the plates. The Hall current is taken into consideration while the induced magnetic field is neglected by assuming a very small magnetic Reynolds number [5]. The two plates are kept at two different but constant temperatures. This configuration is a good approximation of some practical situations such as heat exchangers, flow meters, and pipes that connect system components. The Joule and viscous dissipations are taken into consideration in the energy equation. The governing momentum and energy equations are solved numerically using the finite difference approximations. The inclusion of the Hall current, the suction and injection, and the non-Newtonian fluid characteristics lead to some interesting effects on both the velocity and temperature fields.

2. Formulation of the problem

The geometry of the problem is shown in Fig. 1. The fluid is assumed to be laminar, incompressible and obeying a Casson model and flows between two infinite horizontal plates located at the $y = \pm h$ planes and extend from $x = 0$ to ∞ and from $z = 0$ to ∞. The upper plate is suddenly set into motion and moves with a uniform velocity U_0 while the lower plate is stationary. The upper plate is simultaneously subjected to a step change in temperature from T_1 to T_2. Then, the upper and lower plates are kept at two constant temperatures T_2 and T_1 respectively, with $T_2 > T_1$. The fluid is acted upon by a constant pressure gradient dp/dx in the x-direction, and a uniform suction from above and injection from below which are applied at $t = 0$. A uniform magnetic field $\mathbf{B}_0$ is applied in the positive y-direction and is assumed undisturbed as the induced magnetic field is neglected by assuming a very small magnetic Reynolds number. The Hall effect is taken into consideration and consequently a z-component for the velocity is expected to arise. The uniform suction implies that the y-component of the velocity is constant. Thus, the fluid velocity vector is given by,

$$\mathbf{v}(y,t) = u(y,t)\mathbf{i} + \nu_0\mathbf{j} + w(y,t)\mathbf{k}.$$

The fluid motion starts from rest at $t = 0$, and the no-slip condition at the plates implies that the fluid velocity has neither a z nor an x-component at $y = \pm h$. The initial temperature of the fluid is assumed to be equal to T_1. Since the plates are infinite in the x and z-directions, the physical quantities do not change in these directions.

The flow of the fluid is governed by the momentum equation

$$\rho \frac{D\mathbf{v}}{Dt} = \nabla \cdot (\mu \nabla \mathbf{v}) - \nabla p + \mathbf{J} \times \mathbf{B}_0, \tag{1}$$

where ρ is the density of the fluid and μ is the apparent viscosity of the model and is given by

$$\mu = \left[K_c + \left(\tau_0 / \sqrt{\left(\frac{\partial u}{\partial y}\right)^2 + \left(\frac{\partial w}{\partial y}\right)^2} \right)^{1/2} \right]^2, \tag{2}$$

where K_c^2 is the Casson's coefficient of viscosity and τ_0 is the yield stress. If the Hall term is retained, the current density $\mathbf{J}$ is given by

$$\mathbf{J} = \sigma[\mathbf{v} \times \mathbf{B}_0 - \beta(\mathbf{J} \times \mathbf{V}_0)], \tag{3}$$

where σ is the electric conductivity of the fluid and β is the Hall factor [5]. Equation (3) may be solved in $\mathbf{J}$ to yield

$$\mathbf{J} \times \mathbf{B}_0 = -\frac{\sigma B_0^2}{1 + m^2} [(u + mw)\mathbf{i} + (w - mu)\mathbf{k}], \tag{4}$$

where m is the Hall parameter and $m = \sigma\beta\mathbf{B}_0$. Thus, the two components of the momentum Eq. (1) read

$$\rho \frac{\partial u}{\partial t} + \rho\nu_0 \frac{\partial u}{\partial y} = -\frac{dp}{dx} + \frac{\partial}{\partial y}\left(\mu \frac{\partial u}{\partial y}\right) - \frac{\sigma B_0^2}{1 + m^2}(u + mw), \tag{5}$$

$$\rho \frac{\partial w}{\partial t} + \rho\nu_0 \frac{\partial w}{\partial y} = \frac{\partial}{\partial y}\left(\mu \frac{\partial w}{\partial y}\right) - \frac{\sigma B_0^2}{1 + m^2}(w - mu), \tag{6}$$

The energy equation with viscous and Joule dissipations is given by

$$\rho c_p \frac{\partial T}{\partial t} + \rho c_p \nu_0 \frac{\partial T}{\partial y} = k \frac{\partial^2 T}{\partial y^2} + \mu \left[\left(\frac{\partial u}{\partial y}\right)^2 + \left(\frac{\partial w}{\partial y}\right)^2 \right] + \frac{\sigma B_0^2}{1 + m^2}(u^2 + w^2), \tag{7}$$

where c_p and k are, respectively, the specific heat capacity and the thermal conductivity of the fluid. The second and third terms on the right-hand side represent the viscous and Joule dissipations respectively. We notice that each of these terms has two components. This is because the Hall effect brings about a

velocity w in the z-direction. The initial and boundary conditions of the problem are given by

$$u = w = 0 \text{ at } t < 0, \text{ and } w = 0 \text{ at } y = -h \text{ and } y = h \text{ for } t > 0,$$

$$u = 0 \text{ at } y = -h \text{ for } t \leq 0,\ u = U_0 \text{ at } y = h \text{ for } t > 0, \tag{8}$$

$$T = T_1 \text{ at } t \leq 0,\ T = T_2 \text{ at } y = h \text{ and } T = T_1 \text{ at } y = -h \text{ for } t > 0. \tag{9}$$

It is expedient to write the above equations in the non-dimensional form. To do this, we introduce the following non-dimensional quantities

$$\bar{x} = \frac{x}{h},\ \bar{y} = \frac{y}{h},\ \bar{t} = \frac{tU_0}{h},\ \bar{u} = \frac{u}{U_0},\ \bar{w} = \frac{w}{U_0},\ \bar{p} = \frac{p}{\rho U_0^2},\ \theta = \frac{T - T_1}{T_2 - T_1},\ \bar{\mu} = \frac{\mu}{K_c^2},$$

$\tau_D = \dfrac{\tau_0 h}{K_c^2 U_0}$ is the Casson number (dimensionless yield stress)

$\mathrm{Re} = \dfrac{\rho U_0 h}{K_c^2}$ is the Reynolds number,

$\$ = \dfrac{\rho \nu_0 h}{K_c^2}$ is the suction parameter,

$\mathrm{Pr} = \dfrac{\rho c_p U_0 h}{k}$ is the Prandtl number,

$\mathrm{Ec} = \dfrac{U_0 K_c^2}{\rho c_p h (T_2 - T_1)}$ is the Eckert number,

$Ha^2 = \dfrac{\sigma B_0^2 h^2}{K_c^2}$ is the Hartmann number squared

In terms of the above non-dimensional variables and parameters Eqs.(5)-(9) and (2) are, respectively, written as (where the hats are dropped for convenience);

$$\frac{\partial u}{\partial t} + \frac{\$}{\mathrm{Re}} \frac{\partial u}{\partial y} = -\frac{dp}{dx} + \frac{1}{\mathrm{Re}} \left[\frac{\partial}{\partial y} \left(\mu \frac{\partial u}{\partial y} \right) - \frac{Ha^2}{1 + m^2} (u + mw) \right], \tag{10}$$

$$\frac{\partial w}{\partial t} + \frac{\$}{\mathrm{Re}} \frac{\partial w}{\partial y} = \frac{1}{\mathrm{Re}} \left[\frac{\partial}{\partial y} \left(\mu \frac{\partial w}{\partial y} \right) - \frac{Ha^2}{1 + m^2} (w - mu) \right], \tag{11}$$

$$\frac{\partial \theta}{\partial t} + \frac{\$}{\mathrm{Re}} \frac{\partial \theta}{\partial y} = \frac{1}{\mathrm{Pr}} \frac{\partial^2 \theta}{\partial y^2} + \mathrm{Ec}\, \mu \left[\left(\frac{\partial u}{\partial y} \right)^2 + \left(\frac{\partial w}{\partial y} \right)^2 \right] + \frac{Ha^2 \mathrm{Ec}}{1 + m^2} (u^2 + w^2), \tag{12}$$

$$u = w = 0 \text{ for } t \leq 0 \text{ and } u = w = 0 \text{ at } y = -1,$$
$$w = 0,\ u = 1 \text{ at } y = 1 \text{ for } t > 0, \tag{13}$$

$$\theta = 0 \text{ for } t \leq 0 \text{ and } \theta = 0 \text{ at } y = -1,\ \theta = 1 \text{ at } y = 1 \text{ for } t > 0, \tag{14}$$

$$\mu = \left[1 + \left(\tau_D / \sqrt{\left(\frac{\partial u}{\partial y} \right)^2 + \left(\frac{\partial w}{\partial y} \right)^2} \right)^{1/2} \right]. \tag{15}$$

The shear stress at the two walls is given by

$$\tau_w = \left[\left(\left(\frac{\partial u}{\partial y}\right)^2 + \left(\frac{\partial w}{\partial y}\right)^2\right)^{1/4} + \tau_D^{1/2} \Big/ \left(\left(\frac{\partial u}{\partial y}\right)^2 + \left(\frac{\partial w}{\partial y}\right)^2\right)^{1/4}\right]^2 \Big| y = \pm 1.$$

The Nusselt number at the stationary wall is given by

$$Nu_1 = \frac{2\dfrac{\partial \theta}{\partial y}\Big| y = -1}{-\theta_m}\,.$$

The Nusselt number at the upper moving wall is given by

$$Nu_2 = \frac{2\dfrac{\partial \theta}{\partial y}\Big| y = 1}{1-\theta_m}\,.$$

3. Numerical solution

Equations (10), (11) and (15) represent coupled system of non-linear partial differential equations which are solved numerically under the initial and boundary conditions (13) using the finite difference approximations. A linearization technique is first applied to replace the nonlinear terms at a linear stage, with the corrections incorporated in subsequent iterative steps until convergence is reached. Then the Crank-Nicolson implicit method is used at two successive time levels [17]. An iterative scheme is used to solve the linearized system of difference equations. The solution at a certain time step is chosen as an initial guess for next time step and the iterations are continued till convergence, within a prescribed accuracy. Finally, the resulting block tridiagonal system is solved using the generalized Thomas-algorithm [17]. The energy Eq. (12) is a linear inhomogeneous second-order ordinary differential equation whose right-hand side is known from the solutions of the flow Eqs. (10), (11) and (15) subject to the conditions (13). The values of the velocity components are substituted in the right-hand side of Eq. (12) which is solved numerically with the initial and boundary conditions (14) using central differences for the derivatives and Thomas-algorithm for the solution of the set of discritized equations. Finite difference equations relating the variables are obtained by writing the equations at the mid point of the computational cell and then replacing the different terms by their second order central difference approximations in the y-direction. The diffusion terms are replaced by the average of the central differences at two successive time-levels. The computational domain is divided into meshes each of dimension Δt and Δy in time and space respectively as shown in Fig. 2. We define the variables $\nu = u_y$, $B = w_y$,

$H = \theta_y$ and $\mu' = \mu_y$ to reduce the second order differential Eqs. (10), (11) and (12) to first order differential equations. The finite difference representations for the resulting first order differential Eqs. (10) and (11) together the equations defining the new variables take the form

$$
\begin{aligned}
(16)\quad & \left(\frac{u_{i+1,j+1}-u_{i,j+1}+u_{i+1,j}-u_{i,j}}{2\Delta t}\right)+\frac{\$}{\mathrm{Re}}\left(\frac{v_{i+1,j+1}+v_{i,j+1}+v_{i+1,j}+v_{i,j}}{2\Delta t}\right)\\
&=-\frac{dp}{dx}+\left(\frac{\bar{\mu}_{i,j+1}+\bar{\mu}_{i,j}}{2\,\mathrm{Re}}\right)\left(\frac{(v_{i+1,j+1}+v_{i,j+1})-(v_{i+1,j}+v_{i,j})}{2\Delta y}\right)\\
&+\left(\frac{\bar{\mu}'_{i,j+1}+\bar{\mu}'_{i,j}}{2\mathrm{Re}}\right)\left(\frac{v_{i+1,j+1}+v_{i,j+1}+v_{i+1,j}+v_{i,j}}{4}\right)\\
&-\frac{Ha^2}{1+m^2}\left(\frac{u_{i+1,j+1}+u_{i,j+1}+u_{i+1,j}-u_{i,j}}{4\mathrm{Re}}\right.\\
&\left.+\,m\,\frac{w_{i+1,j+1}+w_{i,j+1}+w_{i+1,j}+w_{i,j}}{4\mathrm{Re}}\right),
\end{aligned}
$$

$$
\begin{aligned}
(17)\quad & \left(\frac{w_{i+1,j+1}-w_{i,j+1}+w_{i+1,j}-w_{i,j}}{2\Delta t}\right)+\frac{\$}{\mathrm{Re}}\left(\frac{B_{i+1,j+1}+B_{i,j+1}+B_{i+1,j}+B_{i,j}}{4}\right)\\
&=\left(\frac{\bar{\mu}_{i,j+1}+\bar{\mu}_{i,j}}{2\,\mathrm{Re}}\right)\left(\frac{(B_{i+1,j+1}+B_{i,j+1})-(B_{i+1,j}+B_{i,j})}{2\Delta y}\right)\\
&+\left(\frac{\bar{\mu}'_{i,j+1}+\bar{\mu}'_{i,j}}{2\mathrm{Re}}\right)\left(\frac{B_{i+1,j+1}+B_{i,j+1}+B_{i+1,j}+B_{i,j}}{4}\right)\\
&+\frac{Ha^2}{1+m^2}\left(m\,\frac{u_{i+1,j+1}+u_{i,j+1}+u_{i+1,j}+u_{i,j}}{4\mathrm{Re}}\right.\\
&\left.-\frac{w_{i+1,j+1}+w_{i,j+1}+w_{i+1,j}+w_{i,j}}{4\mathrm{Re}}\right).
\end{aligned}
$$

The variables with bars are given initial guesses from the previous time steps and an iterative scheme is used at every time to solve the linearized system of difference equations. Then the finite difference form for the energy Eq. (12) can be written as

$$
\begin{aligned}
(18)\quad & \left(\frac{\theta_{i+1,j+1}-\theta_{i,j+1}+\theta_{i+1,j}-\theta_{i,j}}{2\Delta t}\right)+\frac{\$}{\mathrm{Re}}\left(\frac{H_{i+1,j+1}+H_{i,j+1}+H_{i+1,j}+H_{i,j}}{4}\right)\\
&=\frac{1}{\mathrm{Pr}}\left[\frac{(H_{i+1,j+1}+H_{i,j+1})-(H_{i+1,j}+H_{i,j})}{2\Delta y}\right]+DISP,
\end{aligned}
$$

$$\left(\frac{v_{i+1,j+1}+v_{i,j+1}+v_{i+1,j}+v_{i,j}}{4}\right)=\frac{(u_{i+1,j+1}+u_{i,j+1})-(u_{i+1,j}+u_{i,j})}{2\Delta y}, \tag{19}$$

$$\left(\frac{B_{i+1,j+1}+B_{i,j+1}+B_{i+1,j}+B_{i,j}}{4}\right)=\frac{(w_{i+1,j+1}+w_{i,j+1})-(w_{i+1,j}+w_{i,j})}{2\Delta y}, \tag{20}$$

$$\left(\frac{H_{i+1,j+1}+H_{i,j+1}+H_{i+1,j}+H_{i,j}}{4}\right)=\frac{(\theta_{i+1,j+1}+\theta_{i,j+1})-(\theta_{i+1,j}+\theta_{i,j})}{2\Delta y}, \tag{21}$$

where $DISP$ represents the Joule and viscous dissipation terms which are known from the solution of the momentum equations and can be evaluated at the mid point $(i+1/2, j+1/2)$ of the computational cell. Computations have been made for $dp/dx = 5$, Pr=1, Re=1, and Ec=0.2. Grid-independence studies show that the computational domain $0 < t < \infty$ and $-1 < y < 1$ can be divided into intervals with step sizes $\Delta t = 0.0001$ and $\Delta y = 0.005$ for time and space respectively. Smaller step sizes do not show any significant change in the results. Convergence of the scheme is assumed when all of the unknowns u, v, w, B, θ and H for the last two approximations differ from unity by less than 10^{-6} for all values of y in $-1 < y < 1$ at every time step. Less than 7 approximations are required to satisfy this convergence criteria for all ranges of the parameters studied here. In order to examine the accuracy and correctness of the solutions, the results for the non-magnetic and Newtonian cases are compared and shown to have complete agreement with those reported by Attia [10]. This ensures the satisfaction of all the governing equations; mass continuity, momentum and energy equations.

4. Results and discussion

Figures 3, 4 and 5 present the profiles of the velocity components u and w and the temperature θ respectively for various values of time t and for $\tau_D = 0.0$, 0.05, and 0.1. The figures are evaluated for $Ha = 3$, $m = 3$, and \$ = 1. It is clear from Figs. 3 and 4 that increasing the yield stress τ_D decreases the velocity components u and w and the time at which they reach their steady state values as a result of increasing the viscosity. The figures show also that the velocity components u and w do not reach their steady state monotonically. Both u and w increase with time up till a maximum value and then decrease up to the steady state. This behaviour is more pronounced for small values of the parameter τ_D and it is more clear for u than for w. Figure 5 shows that the temperature profile reaches its steady state monotonically. It is observed also that the velocity component u reaches the steady state faster than w which, in turn, reaches the steady state faster than θ . This is expected as u is the source of w, while both u and w act as sources for the temperature.

Figures 6, 7, and 8 depict the variation of the velocity components u and w and the temperature θ at the centre of the channel $(y = 0)$ with time respectively for various values of the Hall parameter m and for $\tau_D = 0.0$, 0.05, and 0.1. In

these figures, $Ha = 3$ and \$ = 1. Figure 6 shows that u increases with increasing m for all values of τ_D as the effective conductivity ($= \sigma/(1+m^2)$) decreases with increasing m which reduces the magnetic damping force on u . It is observed also from the figure that the time at which u reaches its steady state value increases with increasing m while it decreases when τ_D increases. The effect of τ_D on u becomes more pronounced for large values of m. In Fig. 7, the velocity component w increases with increasing m as w is a result of the Hall effect. On the other hand, at small times, w decreases when m increases. This happens due to the fact that, at small times w is very small and then the source term of w is proportional to $(mu/(1+m^2))$ which decreases with increasing m ($m > 1$). This accounts for the crossing of the curves of w with t for all values of τ_D. Figures 6 and 7 indicate also that the influence of τ_D on u and w depends on m and becomes more clear when m is large. An interesting phenomenon is observed in Figs. 6 and 7, which is that, when m has a nonzero value the component u and, sometimes, w overshoot. For some times they exceed their steady state values and then go down towards steady state. This may be explained by stating that with the progress of time, u increases and consequently w increases according to Eq. (11) until w reaches its maximum value. The increase in w results in a small decrease in u according to Eq. (10). This reduction in u may, in turn, result in a decrease in w according to Eq. (11) which explains the reduction after the peaks. The time at which overshooting occurs decreases with increasing τ_D. Figure 8 shows that the influence of m on θ depends on t . Increasing m decreases θ at small times and increases it at large times. This is due to the fact that, for small times, u and w are small and an increase in m increases u but decreases w. Then, the Joule dissipation which is also proportional to $(1/1+m^2)$ decreases. For large times, increasing m increases both u and w and, in turn, increases the Joule and viscous dissipations. This accounts for the crossing of the curves of θ with time for all values of τ_D. It is also observed that increasing τ_D increases the temperature θ for small t, but decreases it for large t (see also Table 1 for more clear presentation of these results). This is because increasing τ_D decreases both u and w and their gradients which decreases the Joule and viscous dissipations. Tables 2 and 3 present the effect of the parameters m and τ_D, respectively, on the steady state time of the temperature θ. It is clear that increasing m increases the steady state time of θ while increasing τ_D decreases it. The figure shows also that the time at which θ reaches its steady state value increases with increasing m while it is not greatly affected by changing τ_D.

Table 1. The development of the temperature θ with time t for $Ha = 3$, $m = 5$ and \$ = 1

τ_D	t=0.1	t=0.3	t=0.5	t=0.7	t=0.9	t=1.1	t=1.3	t=1.5	t=1.7
0.0	.0172	.1419	.2634	.3686	.4488	.5035	.5376	.5574	.5680
0.05	.0299	.1675	.2920	.3874	.4530	.4949	.5199	.5345	.5426
0.1	.0384	.1776	.2998	.3899	.4503	.4880	.5105	.5235	.5309

Table 2. The steady state temperature θ at $y = 0$ and its corresponding time for $\tau_D = 0$, \$ $= 1$ and $Ha = 3$.

m	0	1	3
θ	0.440	0.450	0.500
t	2.0	2.25	2.5

Table 3. The steady state temperature θ at $y = 0$ and its corresponding time for $m = 5$, \$ $= 1$ and $Ha = 3$.

τ_D	0.0	0.05	0.1
θ	0.580	0.549	0.536
t	2.45	2.20	2.00

Figures 9, 10, and 11 show the effect of the suction parameter \$ on the time development of the velocity components u and w and the temperature θ at $y = 0$ with time respectively for various values for $\tau_D = 0.0$, 0.05, and 0.1. In these figures, $Ha = 3$ and $m = 3$. Figure 9 shows that u at the centre of the channel decreases with increasing \$ for all values of τ_D due to the convection of the fluid from regions in the lower half to the centre, which has higher fluid speed. Figure 10 shows that w decreases with increasing \$ for all values of τ_D as a result of decreasing u which affects the source term of w . The figure presents also the influence of \$ on the reduction of the overshooting in w especially for small values of τ_D. Figure 11 indicates that increasing \$ decreases the temperature at the centre of the channel for all values of τ_D. This is due to the influence of the convection in pumping the fluid from the cold lower half towards the centre of the channel.

5. Conclusions

The transient Couette flow of a Casson non-Newtonian fluid under the influence of an applied uniform magnetic field is studied considering the Hall effect. The effects of the Casson number τ_D, the Hall parameter m , and the suction parameter \$ on the velocity and temperature distributions are studied. The Hall term affects the main velocity component u in the x-direction and gives rise to another velocity component w in the z-direction. An overshooting in the velocity components u and w with time due to the Hall effect is observed for all values of τ_D. The flow index τ_D has an apparent effect in controlling the overshooting in u or w and the time at which it occurs. The results show that the influence of the parameter τ_D on u and w depends on m and becomes more apparent when m is large. It is found also that the effect of m on w depends on t for all values of τ_D which accounts for a crossover in the $w - t$ graph for various values of m. The effect of m on the magnitude of θ depends on n and becomes more pronounced in case of small τ_D. The time at which u and w reach the steady state increases with increasing m, but decreases when τ_D increases. The time at which θ reaches its steady state increases with increasing m while it is not greatly affected by changing τ_D.

References

[1] Tao, I.N., *Magnetohydrodynamic effects on the formation of Couette flow*, J. of Aerospace Sci., vol. 27 (1960), 334.

[2] Nigam, S.D. and Singh, S.N., *Heat transfer by laminar flow between parallel plates under the action of transverse magnetic field*, Quart. J. Mech. Appl. Math., vol. 13 (1960), 85.

[3] Alpher, R.A., *Heat transfer in magnetohydrodynamic flow between parallel plates*, Int. J. Heat and Mass Transfer, Vol. 3, pp. 108, 1961.

[4] Tani, I., *Steady motion of conducting fluids in channels under transverse magnetic fields with consideration of Hall effect*, J. of Aerospace Sci., vol. 29 (1962), 287.

[5] Sutton, G.W. and Sherman, A., *Engineering Magnetohydrodynamics*, McGraw-Hill, 1965.

[6] Soundalgekar, V.M., Vighnesam, N.V. and Takhar, H.S., *Hall and Ion-slip effects in MHD Couette flow with heat transfer*, IEEE Transactions on Plasma Science, vol. PS-7, no. 3 (Sept. 1979), 178-182.

[7] Soundalgekar, V.M. and Uplekar, A.G., *Hall effects in MHD Couette flow with heat transfer*, IEEE Transactions on Plasma Science, vol. PS-14, no. 5 (Oct. 1986), 579-583.

[8] Abo-El-Dahab, E.M.H., *Effect of Hall currents on some magnetohydrodynamic flow problems*, Master Thesis, Dept. of Maths., Faculty of Science, Helwan University, Egypt, 1993.

[9] Attia, H.A. and Kotb, N.A., *MHD flow between two parallel plates with heat transfer*, ACTA Mechanica, vol. 117 (1996), 215-220.

[10] Attia, H.A., *Hall current effects on the velocity and temperature fields of an unsteady Hartmann flow*, Can. J. Phys., vol. 76 (9) (1998), 739-746.

[11] Casson, N., *A flow equation for pigment oil-suspensions of the printing ink type", in Rheolgy of Disperse Systems* (C.C. Mill, ed.), P. 84. Pergamon Press, London, 1959.

[12] Tamamashi, B., *Consideration of certain hemorheological phenomena from the stand-point of surface chemistry, in Hemorheology* (A.L. Copley, ed.), P. 89, Pergamon Press, London, 1968.

[13] Walawander, W.P., Chen, T.Y. and Cala, D.F., *An aproximate Casson fluid model for tube flow of blood*, Biorheology, 12 (1975), 111.

[14] Batra, R.L. and Jena, B., *Flow of a Casson fluid in a slightly curved tube*, Int. J. Engng. Sci., 29 (1991), 1245.

[15] Das, B. and Batra, R.L., *Secondary flow of a Casson fluid in a slightly curved tube*, Int. J. Non-Linear Mechanics, 28 (5) (1993), 567.

[16] Sayed Ahmed, M.E. and Attia, H.A., *Magnetohydrodynamic flow and heat transfer of a non-Newtonian fluid in an eccentric annulus*, Can. J. Phys., 76 (1998), 391.

[17] Antia, M., *Numerical Methods for Scientists and Engineers*, Tata McGraw-Hill, New Delhi, 1991.

Accepted: 06.10.2006

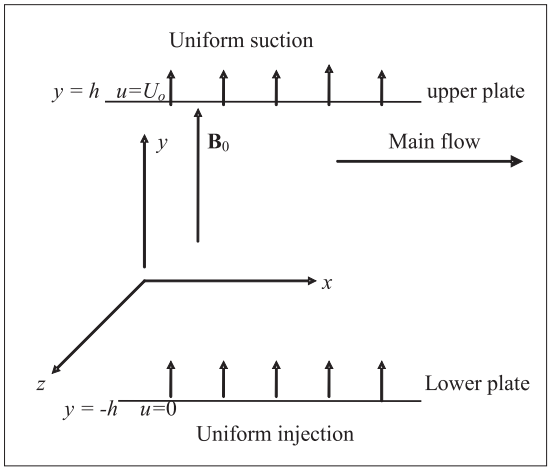

Figure 1: The geometry of the problem

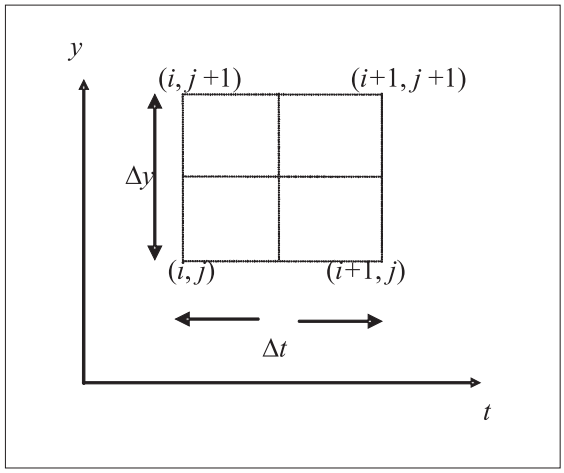

Figure 2: Mesh network

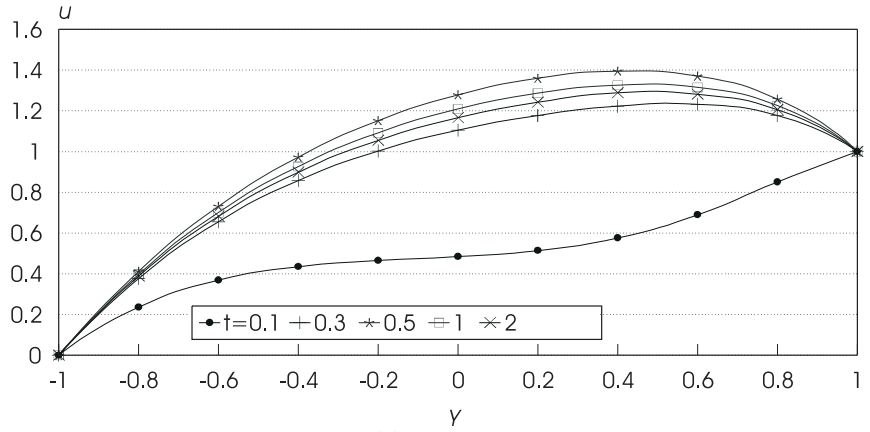

(a) $\tau_D = 0.0$

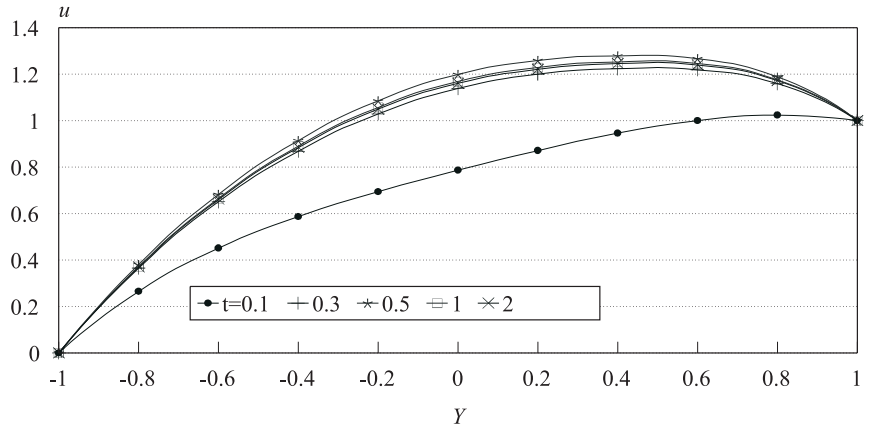

(b) $\tau_D = 0.05$

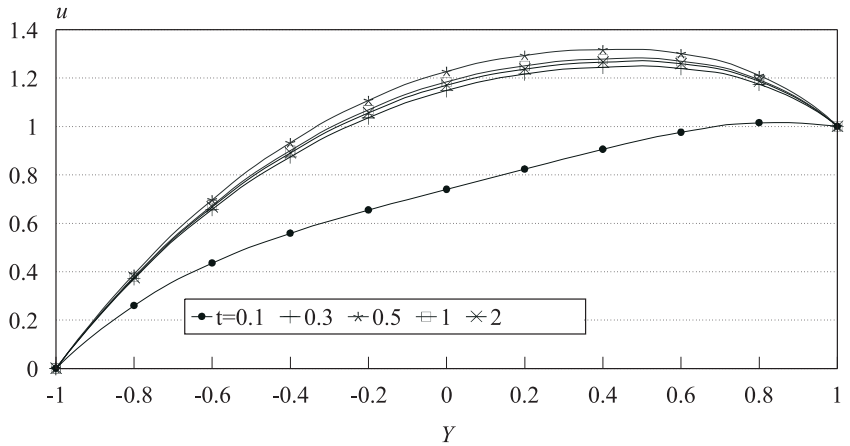

(c) $\tau_D = 0.1$

Figure 3: Time Development of the velocity component u for S=1, Ha=3, m=3.

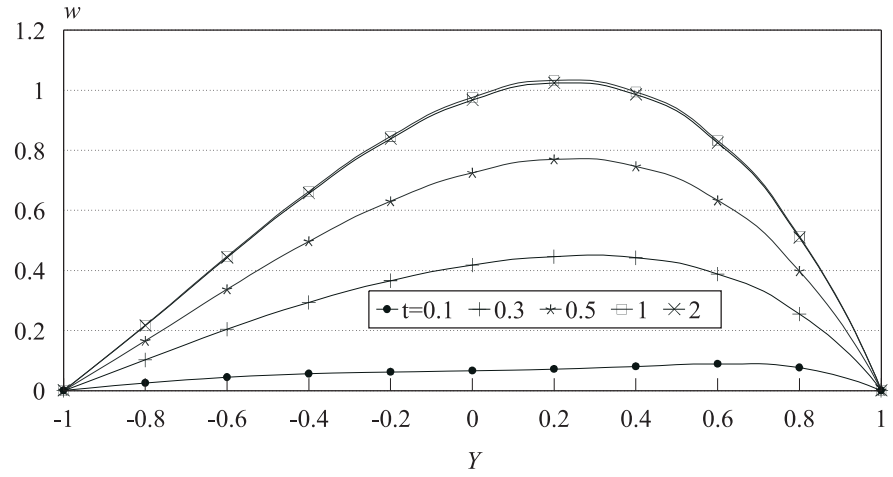

(a) $\tau_D = 0.0$

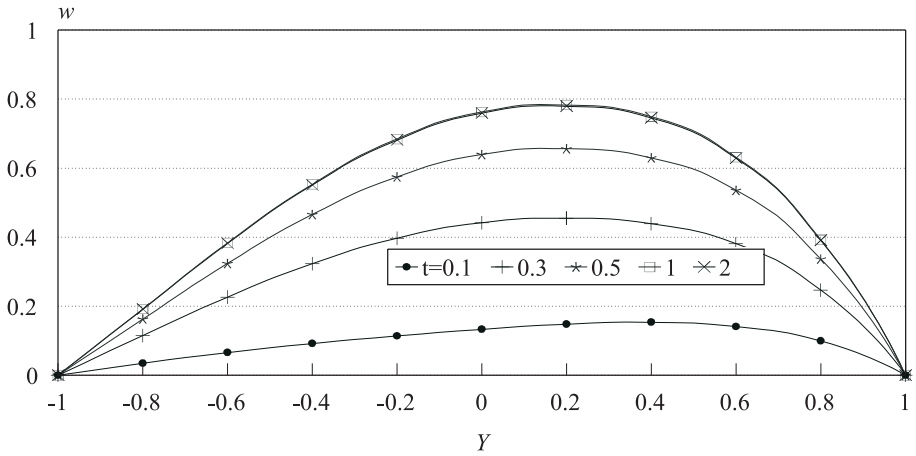

(b) $\tau_D = 0.05$

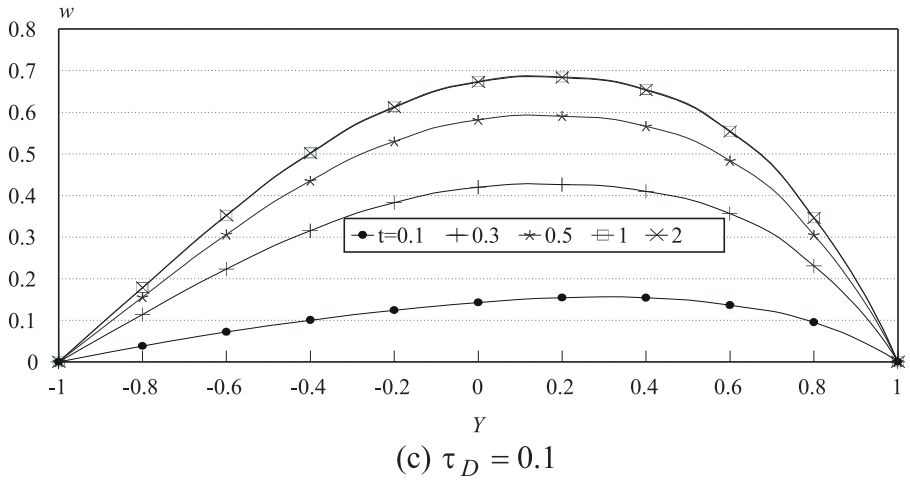

(c) $\tau_D = 0.1$

Figure 4: Time Development of the velocity component w for $S = 1,\ Ha = 3,\ m = 3$.

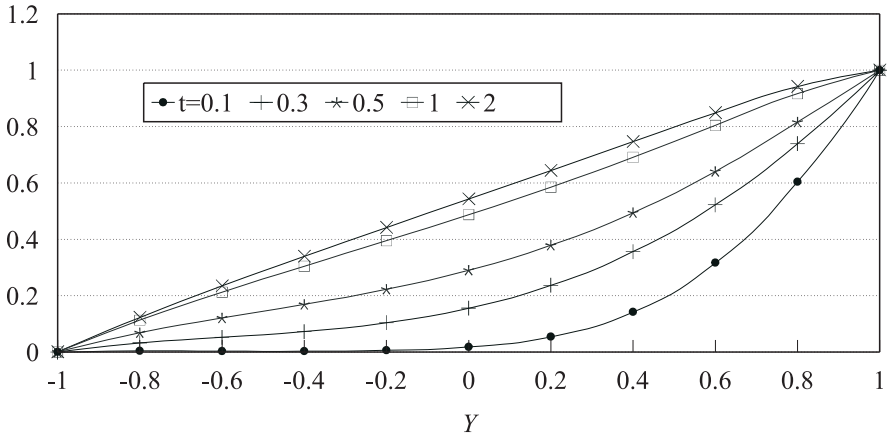

(a) $\tau_D = 0.0$

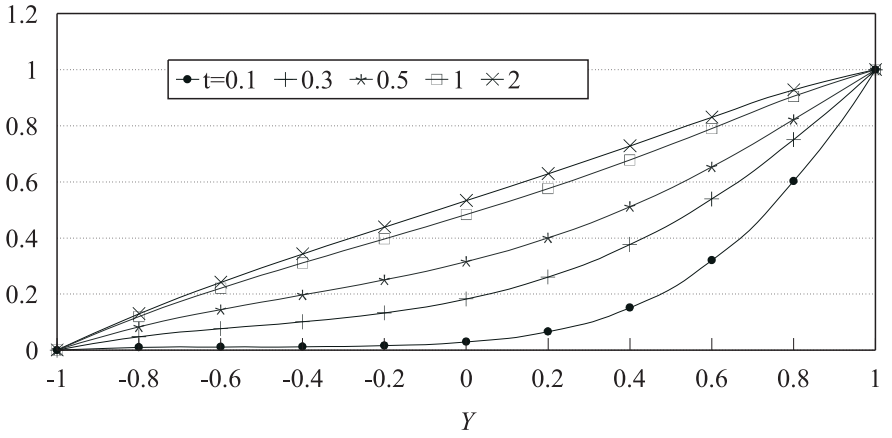

(b) $\tau_D = 0.05$

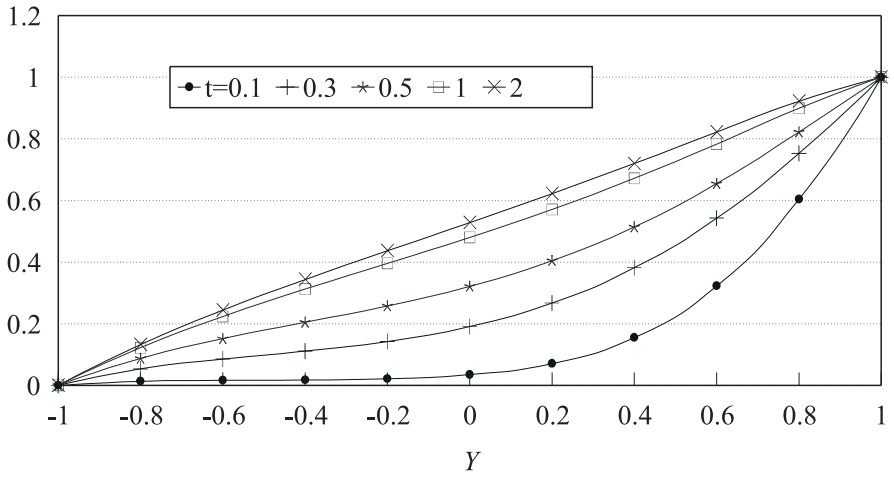

(c) $\tau_D = 0.1$

Figure 5: Time Development of the velocity component θ for $S = 1,\ Ha = 3,\ m = 3$.

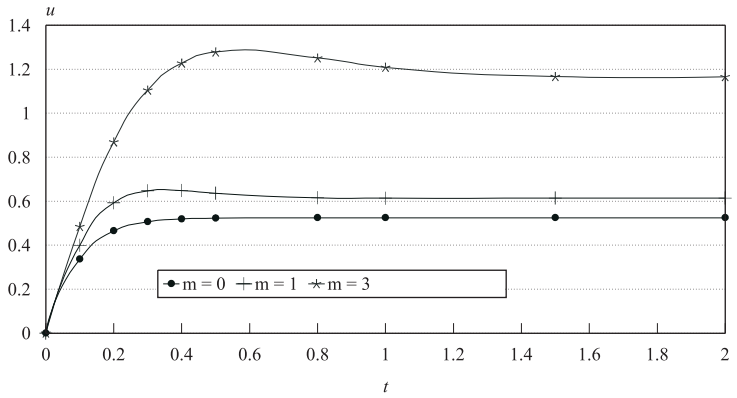

(a) $\tau_D = 0.0$

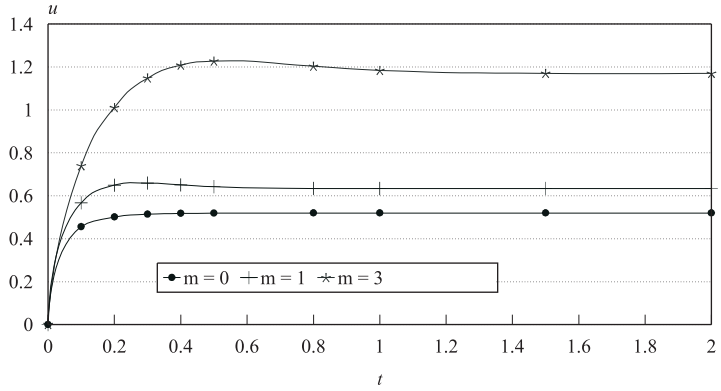

(b) $\tau_D = 0.05$

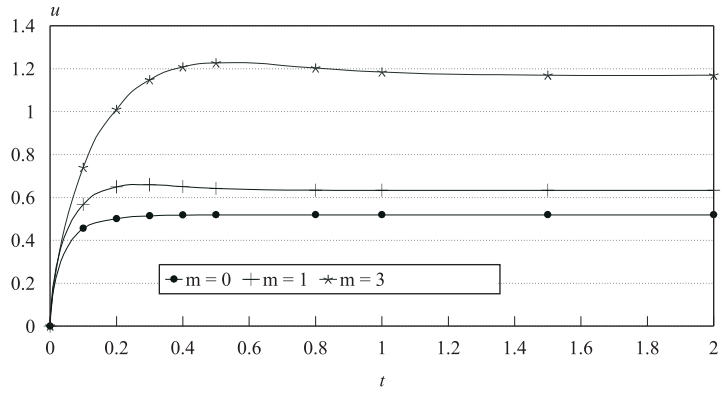

(c) $\tau_D = 0.1$

Figure 6: Effect of the Hall parameter m on the time development of u at $y = 1$ for $S = 1,\ Ha = 3$.

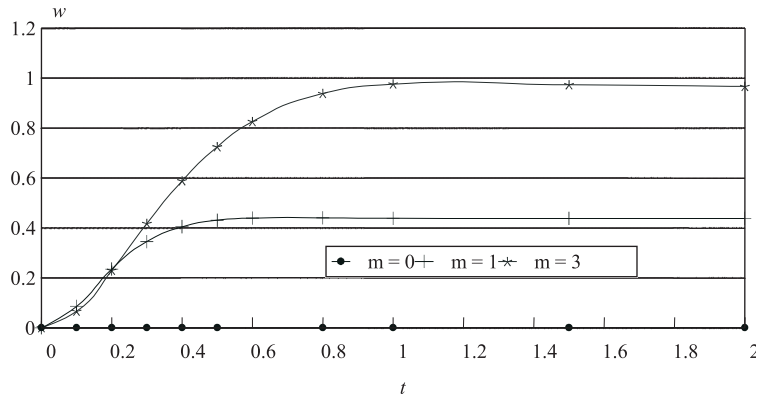

(a) $\tau_D = 0.0$

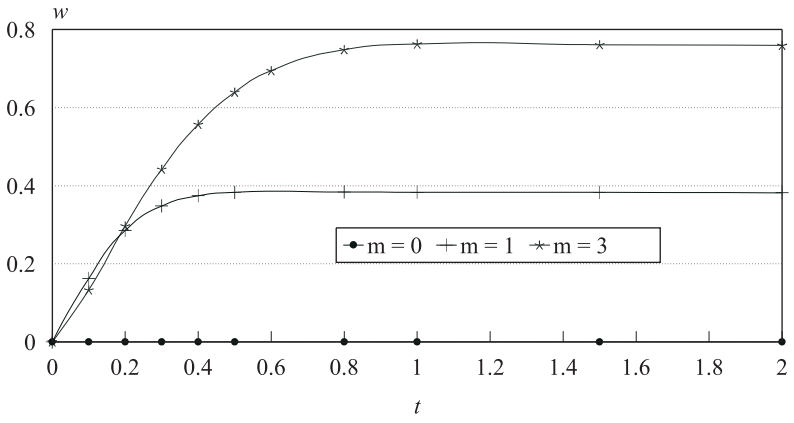

(b) $\tau_D = 0.05$

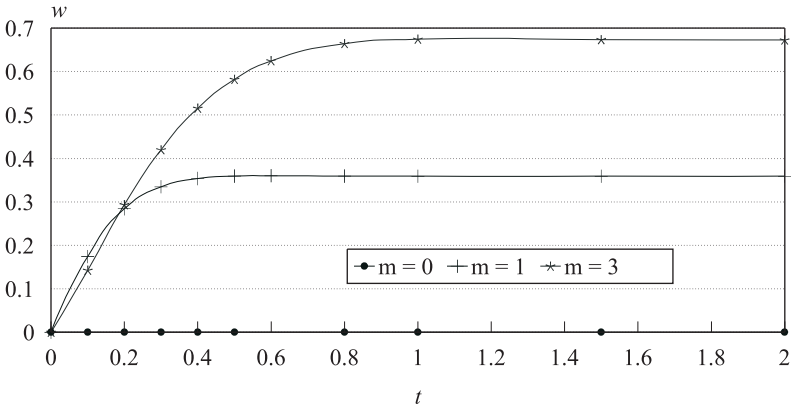

(c) $\tau_D = 0.1$

Figure 7: Effect of the Hall parameter m on the time development of w at $y = 1$ for $S = 1,\ Ha = 3$.

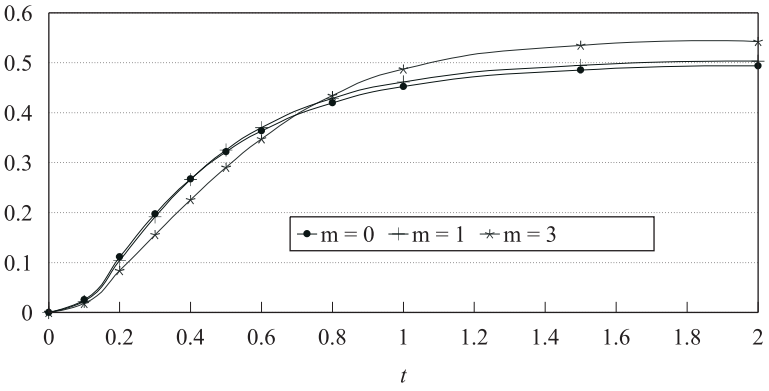

(a) $\tau_D = 0.0$

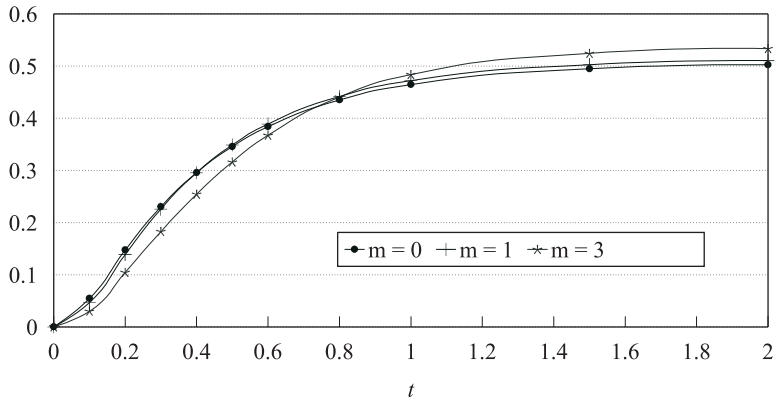

(b) $\tau_D = 0.05$

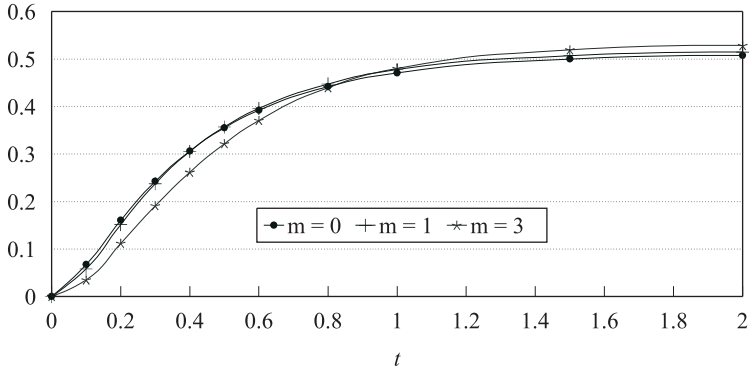

(c) $\tau_D = 0.1$

Figure 8: Effect of the Hall parameter m on the time development of θ at $y = 1$ for $S = 1,\ Ha = 3$.

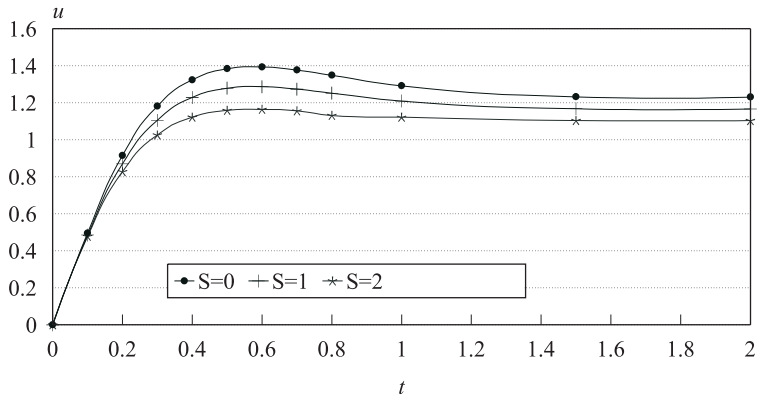

(a) $\tau_D = 0.0$

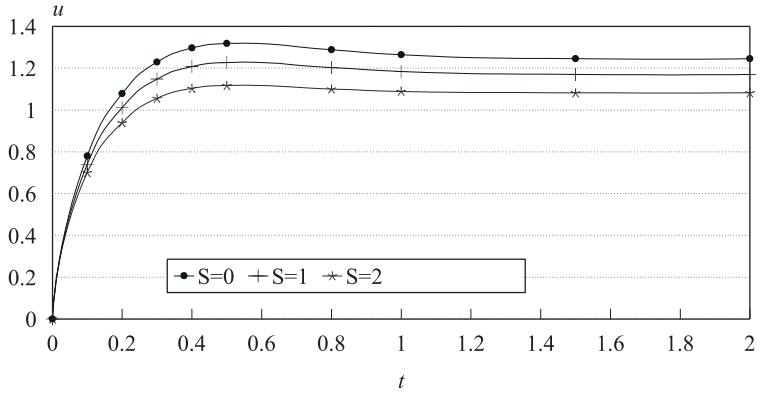

(b) $\tau_D = 0.05$

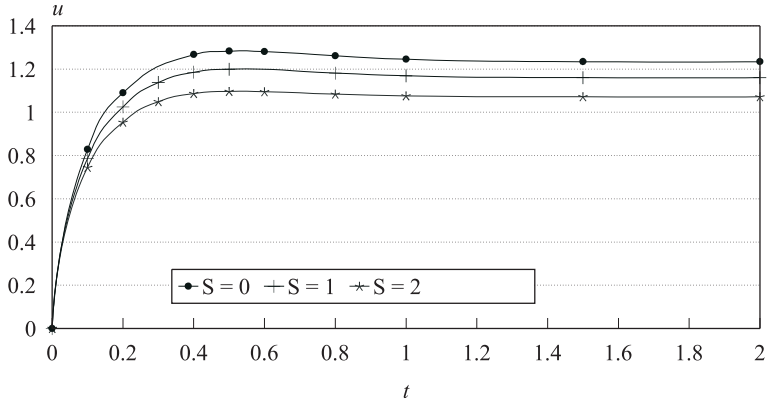

(c) $\tau_D = 0.1$

Figure 9: Effect of the suction parameter S on the time development of u at $y = 1$ for $S = 1,\ Ha = 3$.

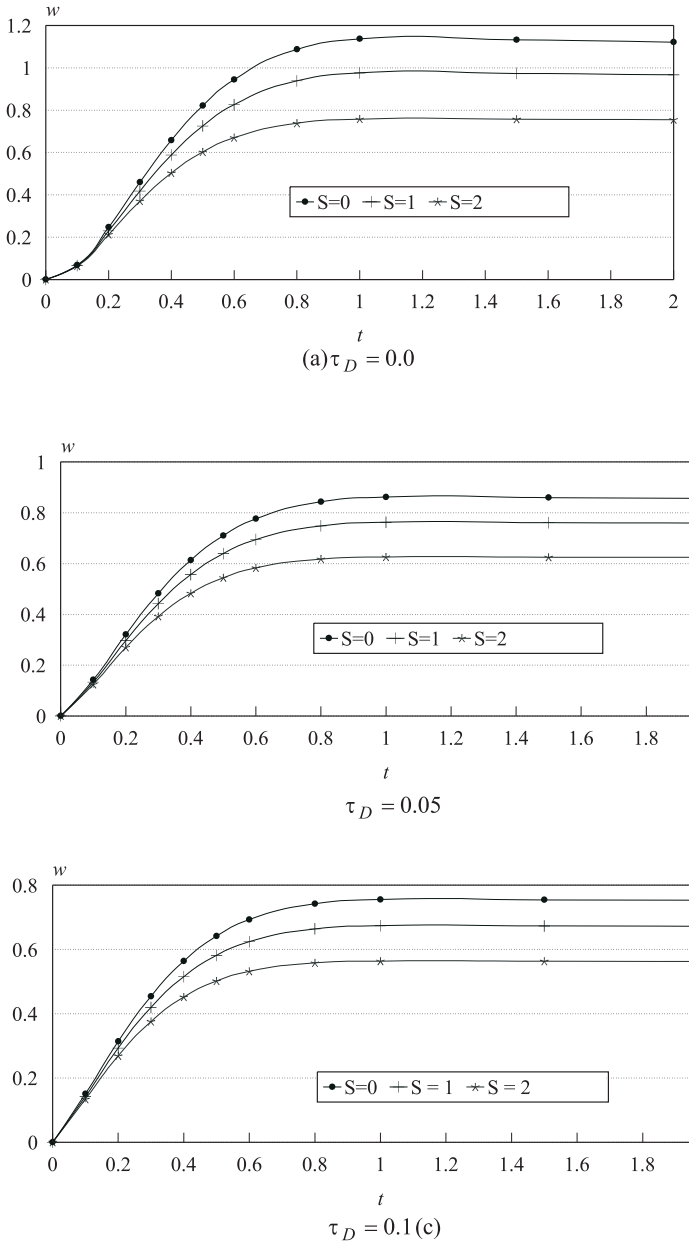

Figure 10: Effect of the suction parameter S on the time development of w at $y = 1$ for $S = 1,\ Ha = 3$.

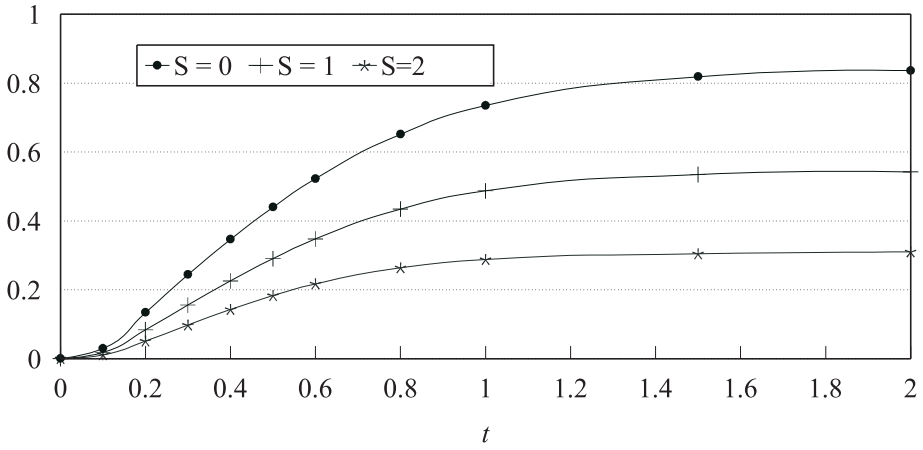

(a) $\tau_D = 0.0$

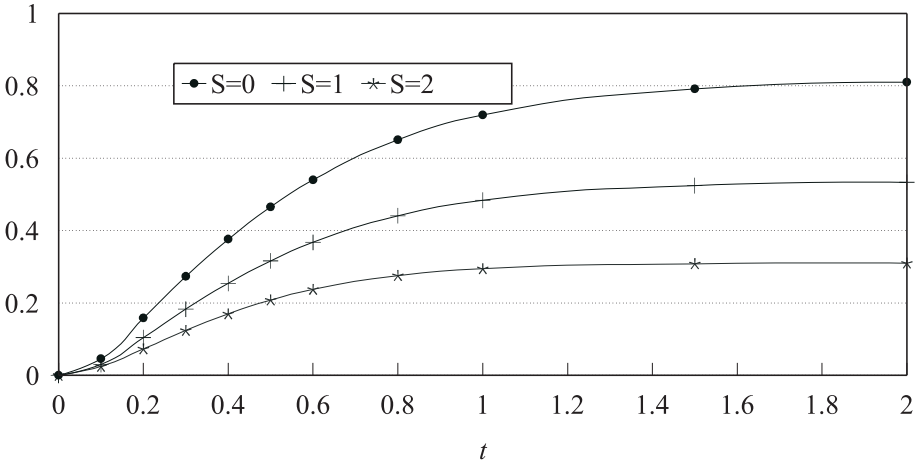

(b) $\tau_D = 0.05$

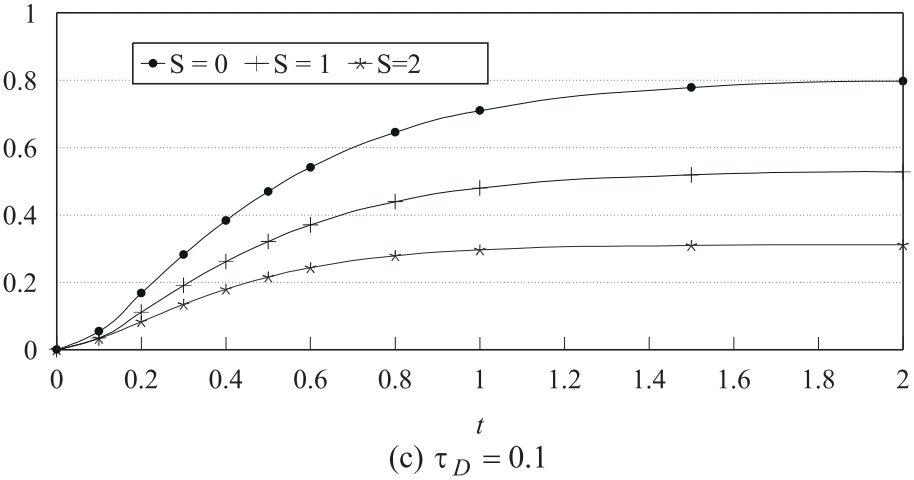

(c) $\tau_D = 0.1$

Figure 11: Effect of the suction parameter S on the time development of θ at $y = 1$ for $S = 1,\ Ha = 3$.